ISBN: 978-3-95450-234-9 ISSN: 2673-5504 doi:10.18429/JACoW-SRF2023-MOPMB019

NUMERICAL CALCULATIONS OF SUPERHEATING FIELD IN SUPERCONDUCTORS WITH NANOSTRUCTURED SURFACES*

W. P. M. R. Pathirana[1†], A. Gurevich[2‡]
[1]Department of Physics and Astronomy, Virginia Military Institute, Lexington, VA, USA,
[2]Department of Physics and Center for Accelerator Science, Old Dominion University, Norfolk, USA

Abstract

We report calculations of a dc superheating field H_{sh} in superconductors with nanostructured surfaces. Particularly, numerical simulations of the Ginzburg-Landau (GL) equations were performed for a superconductor with an inhomogeneous impurity concentration, a thin superconducting layer on top of another superconductor, and S-I-S multilayers. The superheating field was calculated taking into account the instability of the Meissner state with a nonzero wavelength along the surface, which is essential for realistic values of the GL parameter κ. Simulations were done for the materials parameters of Nb and Nb_3Sn at different values of κ and the mean free paths. We show that the impurity concentration profile at the surface and thicknesses of S-I-S multilayers can be optimized to reach H_{sh} exceeding the bulk superheating fields of both Nb and Nb_3Sn. For example, a S-I-S structure with 90 nm thick Nb_3Sn layer on Nb can boost the superheating field up to ≈ 500 mT, while protecting the SRF cavity from dendritic thermomagnetic avalanches caused by local penetration of vortices.

INTRODUCTION

The superconducting radio-frequency (SRF) resonant cavities are crucial components of particle accelerators enabling high accelerating gradients with minimal power consumption. The best Nb cavities can have high quality factors $Q \sim 10^{10} - 10^{11}$ and sustain accelerating fields up to 50 MV/m at $T = 1.5 - 2$ K and $1.3 - 2$ GHz [1, 2]. The peak fields $B_0 \simeq 200$ mT at the equatorial surface of Nb cavities approach the thermodynamic critical field $B_c \approx 200$ mT at which the screening rf current density flowing at the inner cavity surface is close to the depairing current density $J_c \simeq B_c/\mu_0\lambda$ - the maximum dc current density a superconductor can carry in the Meissner state [3], where λ is the London penetration depth. Thus, the breakdown fields of the best Nb cavities have nearly reached the dc superheating field $B_{sh} \simeq B_c$ [4–7]. The Q factors can be increased by materials treatments such as high temperature annealing followed by low temperature baking which not only increase $Q(B_0)$ and the breakdown field but also reduce deterioration of Q at high fields [8, 9]. High temperature treatments combined with the infusion of nitrogen, titanium or oxygen can produce an anomalous increase of $Q(B_0)$ with B_0 [10–13]. These advances raise the question about the fundamental limit of the breakdown fields of SRF cavities and the extent to which it can be pushed by surface nano-structuring and impurity management [2, 14].

Several ways of increasing dc superheating field by surface nanostructuring without detrimental reduction of the field onset of dissipative penetration of vortices have been proposed, including high-T_c superconducting multilayers with thin dielectric layers [15–19] or a dirty overlayer with a higher concentration of nonmagnetic impurities at the surface [20]. Dc superheating field of such structures has been evaluated using the London, Ginzburg-Landau and Usadel equations in the limit of $\kappa \to \infty$ in which the breakdown of the Meissner state at $H = H_{sh}$ occurs uniformly along the planar surface. Yet it has been well established that the breakdown of the Meissner state at $H = H_{sh}$ occurs via a periodic modulation of the order parameter with a wavelength $\sim (\xi^3\lambda)^{1/4}$ along the surface [5, 6]. The effect of such periodic instability on H_{sh} can be particularly important for Nb cavities with $\kappa \sim 1$. Addressing the effect of κ (which in turn depends on the mean free path l) on H_{sh} in superconductors with a nanostructured surface is the goal of this work.

We present results of numerical calculations of H_{sh} for different superconducting geometries in materials with finite κ, and determine the optimal surface nanostructure that can withstand the maximum magnetic field. In particular we consider a bulk superconductor with a thin impurity diffusion layer, a clean superconducting overlayer separated by an insulating layer from the bulk (e.g., Nb_3Sn-I-Nb_3Sn), a thin dirty superconducting layer on top of the same superconductor (e.g., dirty Nb_3Sn-I-clean Nb_3Sn), and a thin high-T_c superconducting layer on top of a low-T_c superconductor (e.g., Nb_3Sn-I-Nb). We calculate H_{sh} and determine the optimal layer thickness for each geometry by numerically solving the Ginzburg-Landau (GL) equations using COMSOL [21].

GINZBURG-LANDAU THEORY AND NUMERICAL CALCULATION OF H_{sh}

We first consider a semi-infinite uniform superconductor in a magnetic field H_0 applied along the z axis, parallel to the planar surface. In this case the GL equations can be reduced to two coupled partial differential equations for the amplitude $\Delta(x, y, t)$ of the complex order parameter $\psi = \Delta e^{i\theta}$ and the z-component of the magnetic field $H(x, y, t)$. It is convenient

* This work was supported by DOE under Grant DE-SC 100387-020 and by Virginia Military Institute (VMI) under Jackson-Hope Grant for faculty travel and Jackson-Hope Funds for New Directions in Teaching and Research Grants (Quantum Initiative in Undergraduate Education at VMI).
† walivepathiranagemr@vmi.edu
‡ gurevich@odu.edu

ISBN: 978-3-95450-234-9 ISSN: 2673-5504 doi:10.18429/JACoW-SRF2023-MOPMB019

to write these equations in the following dimensionless form:

$$\dot{f} - f + f^3 - \nabla^2 f + \frac{\kappa^2}{f^3}\left[(\partial_x h)^2 + (\partial_y h)^2\right] = 0, \quad (1)$$

$$\nabla \cdot \left(\frac{\nabla h}{f^2}\right) = \frac{h}{\kappa^2}. \quad (2)$$

Here $f = \Delta/\Delta_0$, $\Delta_0(T)$ is the equilibrium order parameter in the bulk, $h = H/\sqrt{2}H_c$, all lengths are in units of the coherence length ξ, and $\kappa = \lambda/\xi$ is the GL parameter. Note that, despite the presence of the time derivative $\dot{f}$ in Eqs. (1) and (2), they are in fact quasi-static GL equations but not the true time-dependent GL equations [22, 23] which describe a nonequilibrium superconductor at $T \approx T_c$. Here $\dot{f}$ was added in order to detect the instability of the Merissner state at $H + 0 = H_{sh}$ in numerical simulations upon slow ramping the applied magnetic field $H_0(t)$.

Equations (1) and (2) were solved numerically with the following boundary conditions:

$$\begin{aligned} &h(0, y) = h_0(t), \\ &h(x, 0) = h(x, L_y), f(x, 0) = f(x, L_y), \\ &f(L_x, y) = 1,\ h(L_x, y) = 0, \end{aligned} \quad (3)$$

where $h_0 = H_0/\sqrt{2}H_c$, the lengths L_x and L_y of the simulation box $L_x \times L_y$ were chosen to be $\sim 10^4\xi$. Ramping the magnetic field was implemented by $h_0(t) = \theta(t - t_0)(m_1 t_0 + m_2(t - t_0)) + m_1 t\theta(t_0 - t)$, where $\theta(t)$ is the Heaviside step function, $m_1 = 0.01$, $m_2 = 0.00005$ and t_0 was chosen such that $H_0(t_0) < H_{sh}$.

Shown in Figs. 1(a) - 1(b) are the order parameters $f(x, y)$ calculated at $\kappa = 10$ and the applied field H_0 being slightly below and above H_{sh}. At $H_0 < H_{sh}$ there is a gradual reduction of $f(x)$ by the screening current density at the surface. At $H_0 > H_{sh}$ the stationary distribution of $f(x)$ becomes unstable with respect to growing periodic modulations shown in Fig. 1(b). This instability occurs at a finite wavelength $\lambda_c = 2\pi/k_c$, small disturbance of the order parameter initially growing exponentially with time $\delta f(x, y, t) \propto \delta f(x)e^{ik_c y + \Gamma t}$ with $\Gamma > 0$. When calculating H_{sh}, the program was set to stop at $|f_{max}(0, y) - \bar{f}| \approx 10^{-4}$, where $f_{max}(0, y)$ and $\bar{f}$ are the maximum and averaged values of $f(x, y)$ at the surface $x = 0$. Here λ_c was obtained from the maximum peak in the spatial Fourier transform of $\delta f(0, y)$ shown in Fig. 2. The instability is a precursor of penetration of vortex structure with the initial period $\lambda_c \sim (\xi^3\lambda)^{1/4}$ smaller than the stationary vortex spacing $\sim \sqrt{\lambda\xi}$ at $H_0 \simeq H_{sh}$. Analytical approximation for H_{sh} and k_c at $\kappa \gg 1$ are given by [5, 6]:

$$\frac{H_{sh}}{H_c} \approx \frac{\sqrt{5}}{3} + \frac{0.545}{\kappa}, \quad (4)$$

$$\lambda k_c \approx 0.956\kappa^{3/4}. \quad (5)$$

IMPURITY DIFFUSION LAYER

Consider a dirty layer at the surface with an inhomogeneous impurity concentration as shown in Fig. 3. In our simulations such layer was modeled by a spatially varying coherence length $\xi^2(x)/\xi_\infty^2 = 1 - \alpha\exp(-x/l_d)$, where ξ_∞

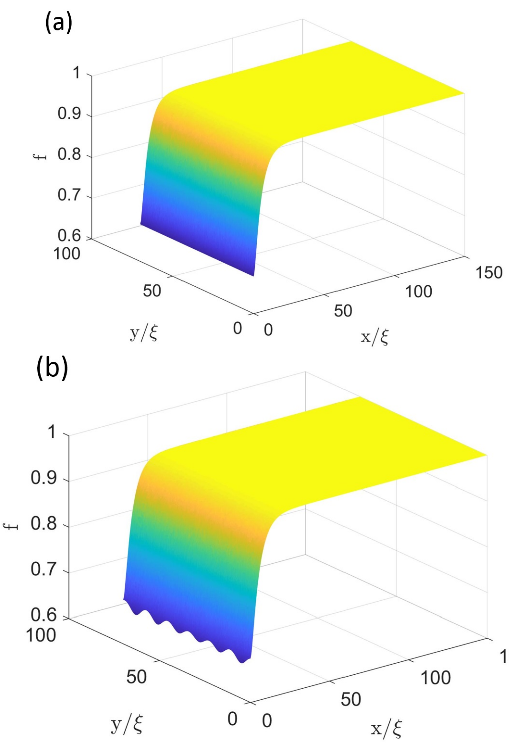

Figure 1: Order parameter calculated at $\kappa = 10$, $H_0 = H_{sh} - 0$ (a) and $H_0 = H_{sh} + 0$ (b).

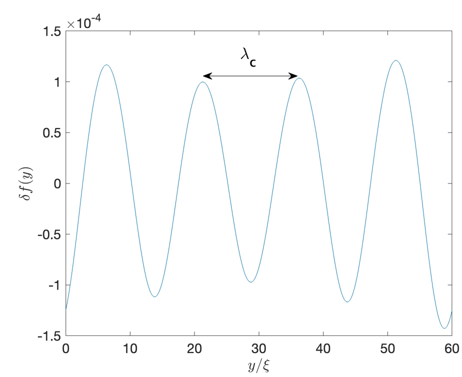

Figure 2: A snapshot of $\delta f(y)$ at $x = 0$ and $H_0 = H_{sh} + 0$.

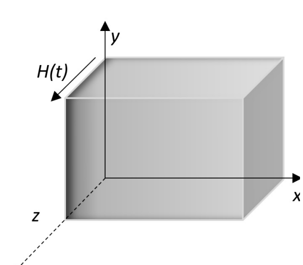

Figure 3: An impurity diffusion layer at the surface shown by the dark gray contrast.

ISBN: 978-3-95450-234-9 ISSN: 2673-5504 doi:10.18429/JACoW-SRF2023-MOPMB019

is a bulk coherence length far away from the surface, l_d is a thickness of the diffusion layer and $\alpha < 1$ quantifies the reduction of $\xi(0) = (1-\alpha)^{1/2}\xi_\infty$ at the surface. The resulting GL equations take the form

$$\dot{f} = f - f^3 + \nabla\cdot\left(S_\gamma \nabla f\right) - \frac{\kappa^2}{S_\gamma f^3}\left[\left(\partial_x h\right)^2 + \left(\partial_y h\right)^2\right], \quad (6)$$

$$\nabla\cdot\left(\frac{\nabla h}{f^2}\right) = \frac{S_\gamma}{\kappa^2}h + \frac{1}{S_\gamma f^2}\left(\partial_x S_\gamma \cdot \partial_x h\right), \quad (7)$$

where $\kappa = \lambda_\infty/\xi_\infty$, $S_\gamma = \xi^2(x)/\xi_\infty^2 = 1 - \alpha\exp(-x/l_d)$, and the lengths are in units of ξ_∞. The boundary conditions are the same as in Eq. (3). Different impurity profiles were investigated by changing α and l_d using $\kappa = 2$ and $\kappa = 10$ as representative values for clean and dirty Nb.

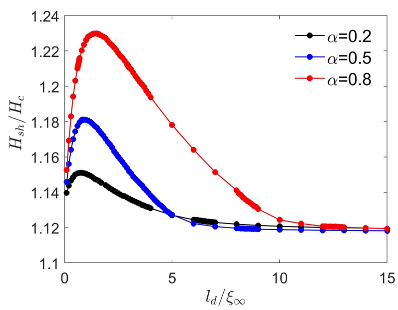

Figure 4: H_{sh} vs l_d for different α at $\kappa = 2$.

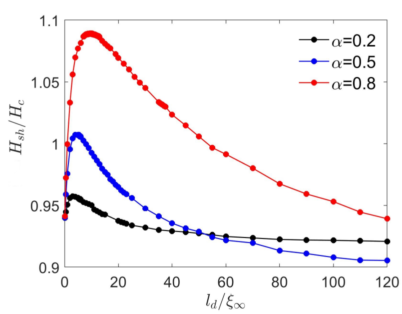

Figure 5: H_{sh} vs l_d for different α at $\kappa = 10$.

The calculated dependencies of $H_{sh}(l_d)$ on the diffusion layer thickness at different α for $\kappa = 2$ and $\kappa = 10$ are shown in Figs. 4 and 5, respectively. One can see that $H_{sh}(l_d)$ first increases with l_d, reaches a maximum and then decreases with l_d approaching a lower value of H_{sh} at $l_d \gg \xi_\infty$. At $\kappa = 2$, $H_{sh}(l_d)$ is maximum at $l_d = 0.8\xi_\infty, 0.9\xi_\infty, 1.5\xi_\infty$ for $\alpha = 0.2, 0.5, 0.8$, respectively. Likewise at $\kappa = 10$ H_{sh} is maximum at $l_d = 4\xi_\infty, 5\xi_\infty, 10\xi_\infty$. Here the diffusion layer can increase H_{sh} by $\approx 9\%$ at $\kappa = 2$ and by $\approx 14\%$ at $\kappa = 10$ as compared to a superconductor with an ideal surface.

S-I-S STRUCTURES

We have considered three different S-I-S structures: an S layer of thickness d separated by an insulator from the S substrate, a thin dirty S layer on top of a cleaner superconductor (e.g., dirty Nb - I - clean Nb) and a thin high T_c overlayer on top of a low T_c superconductor (e.g., Nb_3Sn-I-Nb). Here the I-layer is assumed to be thick enough to fully suppress the Josephson coupling between the S overlayer and the bulk. The geometry is shown in Fig. 6.

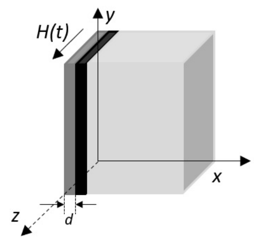

Figure 6: S-I-S geometry. The black line represents and insulating layer while gray and light gray ares represent bulk superconductor and thin superconducting overlayer.

S Overlayer on Top of the Same S-substrate

The GL equations Eqs. (1) and (2) were solved in both S-domains with the boundary conditions (Eq. (3)) supplemented by the conditions of continuity of $h(d+0, y) = h(d-0, y)$ and zero current $\partial_y h(d+0) = \partial_y h(d-0) = 0$ through the I layer.

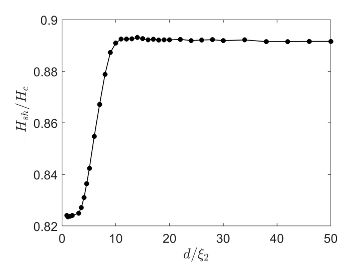

Figure 7: H_{sh} vs d for the case of Nb_3Sn-I-Nb_3Sn,

Shown in Fig. 7 is H_{sh} as a function of the thickness of the S overlayer d calculated at $\kappa = 17$ representing Nb_3Sn. Here $H_{sh}(d)$ is reduced in a very thin S layer and gradually increases with d reaching the bulk value of H_{sh} at $d > 9\xi_2$, where ξ_2 is the coherence length in the S-substrate.

Dirty S Overlayer on S-substrate

Superconductivity in the bulk is described by the following GL equations

$$\dot{f_2} = \nabla^2 f_2 + f_2 - f_2^3 - \frac{\kappa_2^2}{f_2^3}\left[\left(\partial_x h_2\right)^2 + \left(\partial_y h_2\right)^2\right], \quad (8)$$

$$\nabla\cdot\left(\frac{\nabla h_2}{f_2^2}\right) = \frac{h_2}{\kappa_2^2}, \quad (9)$$

where the lengths and the order parameter are in units of their respective bulk values of ξ_2 and Δ_2. In turn, the GL

ISBN: 978-3-95450-234-9 ISSN: 2673-5504 doi:10.18429/JACoW-SRF2023-MOPMB019

equations in the overlayer are:

$$\dot{f}_1 = f_1 - f_1^3 + \frac{\xi_1^2}{\xi_2^2}\nabla^2 f_1 - \frac{\xi_1^2}{\xi_2^2}\frac{\kappa_1^2}{f_1^3}\left[(\partial_x h_1)^2 + (\partial_y h_1)^2\right], \tag{10}$$

$$\nabla \cdot \left(\frac{\nabla h_1}{f_1^2}\right) = \frac{h_1 \xi_2^2}{\xi_1^2 \kappa_1^2}. \tag{11}$$

Equations (8)-(11) were solved for a dirty Nb_3Sn overlayer on a cleaner Nb_3Sn using $l = 2$ nm, $\lambda \approx \lambda_0(\xi_0/l)^{1/2} \approx 135$ nm, $\xi \approx (l\xi_0)^{1/2} \approx 3$ nm, $\kappa_1 = 45$ in the overlayer and $\kappa_2 = 17$ in the bulk Nb_3Sn.

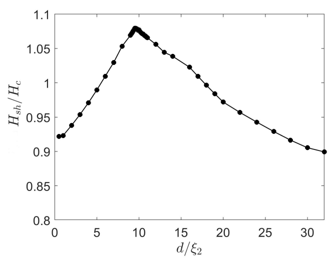

Figure 8: H_{sh} vs d for a Nb_3Sn(dirty)-I-Nb_3Sn structure.

Shown in Fig. 8 is the calculated dependence of H_{sh} on the overlayer thickness which has a maximum at the optimum thickness $d_m \approx 9\xi_2$. Such optimal dirty overlayer can increase H_{sh} by about 10% as compared to the bulk H_{sh}. The behavior of $H_{sh}(d)$ at a finite κ turns out to be similar to that was calculated from the London and GL theories in the limit of $\kappa \to \infty$ in which the enhancement of H_{sh} at $d \simeq d_m$ results from the counterflow induced by the substrate in the overlayer with a larger λ [16, 19]. Here the cusp-like dependence of $H_{sh}(d)$ is controlled by the instability of the Meissner state in the substrate at $d < d_m$ and by the instability of the Meissner state in the overlayer at $d > d_m$, the overlayer partly screening the substrate and allowing it to withstand external fields higher than the bulk H_{sh}.

High-T_c Superconducting Overlayer

A high-T_c superconducting layer on top of a low-T_c substrate is described by the following GL equations

$$\dot{f}_1 = \zeta f_1 - f_1^3 + s\nabla^2 f_1 - \frac{\tilde{\kappa}^2}{f_1^3}\left[(\partial_x h_1)^2 + (\partial_y h_1)^2\right], \tag{12}$$

$$\nabla \cdot \left(\frac{\nabla h_1}{f_1^2}\right) = \frac{\lambda_2^2 h_1}{\lambda_1^2 \zeta \kappa_2^2}, \tag{13}$$

$$\zeta = \frac{1 - T/T_{c1}}{1 - T/T_{c2}}, \qquad s = \frac{\xi_1^2}{\xi_2^2}\zeta, \qquad \tilde{\kappa}^2 = \frac{\xi_1^2 \lambda_1^4}{\xi_2^2 \lambda_2^4}\kappa_2^2 \zeta^3, \tag{14}$$

where T_{c1} and T_{c2} are the critical temperatures of the overlayer and the substrate, respectively. Equations (12)-(14) are supplemented by Eqs. (1) and (2) in the S substrate, the boundary conditions (3) and the conditions of field continuity and zero current through the I layer.

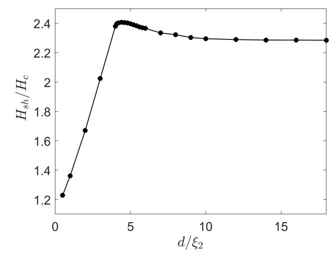

Figure 9: H_{sh} vs d for the case of Nb_3Sn-I-Nb.

We solved the GL equations for a Nb_3Sn overlayer on a bulk Nb using $\kappa_2 = 50/22$ [24] and $\kappa_1 = 17$. The calculated superheating field $H_{sh}(d)$ shown in Fig. 9 has a maximum at $d_m \approx 4\xi_2$. Here $H_{sh}(d)$ at $d < d_m$ is limited by the instability of the Meissner state in Nb partly screened by the Nb_3Sn overlayer, while H_{sh} at $d > d_m$ is determined by the superheating field of Nb_3Sn enhanced at $d_m \approx 88$ nm by the counterflow caused by the Nb substrate. The instability wave vectors k_c in Nb and Nb_3Sn are described reasonably well by Eq. (5). Such Nb_3Sn-I-Nb structure with $d \gtrsim d_m$ can boost the superheating field up to ~ 2.2 times higher than the bulk H_{sh} of Nb. Here the I layer blocks penetration of vortices in the bulk Nb and does not let them develop into thermomagnetic avalanches triggering a global superconductivity breakdown in the cavity.

CONCLUSION

In this work we have used the Ginzburg-Landau theory to study the influence of impurity profiles and high-T_c superconducting layers on the dc superheating field in S-S and S-I-S structures. Unlike the previous calculations of H_{sh} done in the limit of $\kappa \to \infty$, our numerical simulations cover the entire range of $1 < \kappa < \infty$ and account for the instability $H = H_{sh}$ at a finite wave number k_c particularly important for Nb with $\kappa \sim 1$. We show that there are optimum thicknesses of the impurity diffusion layer and the superconducting overlayer which maximize H_{sh}. For instance, optimizing the diffusion length can enhance H_{sh} by $\simeq 5 - 20\%$ at $\kappa = 10$ and by $\simeq 2 - 9\%$ at $\kappa = 2$. An optimized dirty overlayer, such as a Nb_3Sn layer deposited on Nb_3Sn, can enhance the superheating field by $\simeq 10\%$ as compared to H_{sh} of a clean Nb_3Sn. A S-I-S structure comprised of a Nb_3Sn overlayer on Nb can boost the superheating field by approximately 2.2 times as compared to H_{sh} of Nb. A dynamic superheating field at $T \approx T_c$ at rf frequencies can be by a factor $\sqrt{2}$ larger [23] than the quasistatic H_{sh} considered here. The results of this work can contribute to the understanding and optimization of SRF cavities to achieve higher accelerating gradients.

ACKNOWLEDGMENTS

This work was supported by DOE under Grant DE-SC 100387-020 and by Virginia Military Institute (VMI) under Jackson-Hope Grant for faculty travel and Jackson-Hope

ISBN: 978-3-95450-234-9 ISSN: 2673-5504 doi:10.18429/JACoW-SRF2023-MOPMB019

Funds for New Directions in Teaching and Research Grants (Quantum Initiative in Undergraduate Education at VMI).

REFERENCES

[1] H. Padamsee, J. Knobloch, and T. Hays, *RF superconductivity for accelerators.* Second Ed. Wiley, ISBN:978-3-527-40842-9, 2008.

[2] A. Gurevich, "Tuning microwave losses in superconducting resonators", *Supercond. Sci. Technol.*, vol. 36, p. 063002, 2023. doi:10.1088/1361-6668/acc214

[3] M. Tinkham, *Introduction to superconductivity*, Dover Publ., Mineola, NY, USA, 2004.

[4] J. Matricon and D. Saint-James, "Superheating fields in superconductors", *Phys. Lett. A*, vol. 24, pp. 241–242, 1967. doi:10.1016/0375-9601(67)90412-4

[5] S. J. Chapman, "Superheating field of type II superconductors", *SIAM J. Appl. Math.*, vol. 55, pp. 1233–1258, 1995.

[6] M. K. Transtrum, G. Catelani, and J. P. Sethna, "Superheating field of superconductors within Ginzburg-Landau theory", *Phys. Rev. B*, vol. 83, p. 094505, 2011. doi:10.1103/PhysRevB.83.094505

[7] F. P. J. Lin and A. Gurevich, "Effect of impurities on the superheating field of type-II superconductors", *Phys. Rev. B*, vol. 85, p. 054513, 2012. doi:10.1103/PhysRevB.85.054513

[8] G. Ciovati *et al.*, "High field Q slope and the baking effect: Review of recent experimental results and new data on Nb heat treatments", *Phys. Rev. Accel. Beams*, vol. 13, 2010. doi:10.1103/PhysRevSTAB.13.022002

[9] S. Posen, A. Romanenko, A. Grassellino, O. Melnychuk, and D. Sergatskov, "Ultralow surface resistance via vacuum heat treatment of superconducting radio-frequency cavities", *Phys. Rev. Appl.*, vol. 13, no. 1, p. 014024. doi10.1103/PhysRevApplied.13.014024

[10] G. Ciovati, P. Dhakal, and G. R. Myneni, "Superconducting radio-frequency cavities made from medium and low-purity niobium ingots", *Supercond. Sci. Technol.*, vol. 29, p. 064002, 2016. doi:10.1088/0953-2048/29/6/064002

[11] A. Grassellino *et al.*, "Unprecedented quality factors at accelerating gradients up to 45 $\mathrm{MVm^{-1}}$ in niobium superconducting resonators via low temperature nitrogen infusion", *Supercond. Sci. Technol.*, vol. 30, p. 094004, 2017. doi:10.1088/1361-6668/aa7afe

[12] E. M. Lechner, J. W. Angle, F. A. Stevie, M. J. Kelley, C. E. Reece, and A. D. Palczewski, "RF surface resistance tuning of superconducting niobium via thermal diffusion of native oxide", *Appl. Phys. Lett.*, vol. 119, p. 082601, 2021. doi:10.1063/5.0059464

[13] P. Dhakal, "Nitrogen doping and infusion in SRF cavities: A review", *Phys. Open*, vol. 5, p. 100034, 2020. doi:10.1016/j.physo.2020.100034

[14] A. Gurevich and T. Kubo, "Surface impedance and optimum surface resistance of a superconductor with an imperfect surface", *Phys. Rev. B*, vol. 96, p. 184515, 2017. doi:10.1103/PhysRevB.96.184515

[15] A. Gurevich, "Enhancement of rf breakdown field of superconductors by multilayer coating", *Appl. Phys. Lett.*, vol. 88, p. 012511, 2006. doi:10.1063/1.2162264

[16] A. Gurevich, "Maximum screening fields of superconducting multilayer structures", *AIP Adv.*, vol. 5, p. 017112, 2015. doi:10.1063/1.4905711

[17] D. B. Liarte, S. Posen, M. K. Transtrum, G. Catelani, M. Liepe, and J. P. Sethna, "Theoretical estimates of maximum fields in superconducting resonant radio frequency cavities: stability theory, disorder, and laminates", *Supercond. Sci. Technol.*, vol. 30, p. 033002, 2017. doi:10.1088/1361-6668/30/3/033002

[18] T. Kubo, "Multilayer coating for higher accelerating fields in superconducting radio-frequency cavities: a review of theoretical aspects", *Supercond. Sci. Technol.*, vol. 30, p. 023001, 2017. doi:10.1088/1361-6668/30/2/023001

[19] T. Kubo, "Superheating fields of semi-infinite superconductors and layered superconductors in the diffusive limit: structural optimization based on the microscopic theory", *Supercond. Sci. Technol.*, vol. 34, p. 045006, 2021. doi:10.1088/1361-6668/abdedd

[20] V. Ngampruetikorn and J. A. Sauls, "Effect of inhomogeneous surface disorder on the superheating field of superconducting RF cavities", *Phys. Rev. Res.*, vol. 1, p. 012015, 2019. doi:10.1103/PhysRevResearch.1.012015

[21] COMSOL Multiphysics Modeling Software, https://www.comsol.com

[22] R. J. Watts-Tobin, Y. Krähenbühl, and L. Kramer, "Nonequilibrium theory of dirty, current-carrying superconductors: phase-slip oscillators in narrow filaments near T_c", *J. Low Temp. Phys.*, vol. 42, p. 459, 1981. doi:10.1007/BF00117427

[23] A. Sheikhzada and A. Gurevich, "Dynamic pair-breaking current, critical superfluid velocity, and nonlinear electromagnetic response of nonequilibrium superconductors", *Phys. Rev. B*, vol. 102, p. 104507, 2020. doi:10.1103/PhysRevB.102.104507

[24] S. Posen and D. L. Hall, "Nb_3Sn superconducting radiofrequency cavities: fabrication, results, properties, and prospects", *Supercond. Sci. Technol.*, vol. 30, p. 033004, 2017. doi:10.1088/1361-6668/30/3/033004